Therapeutic potential of the prolyl hydroxylase inhibitor roxadustat in a mouse hindlimb lymphedema model

Yoshitada Hoshino, Masayuki Osawa, Emi Funayama, Kosuke Ishikawa, Takahiro Miura, Masahiro Hojo, Yuhei Yamamoto, Taku Maeda

Department of Plastic and Reconstructive Surgery, Faculty of Medicine and Graduate School of Medicine, Hokkaido University, Sapporo, Japan

Running title: THERAPEUTIC POTENTIAL OF ROXADUSTAT FOR LYMPHEDEMA

Corresponding author: Taku Maeda

Department of Plastic and Reconstructive Surgery, Faculty of Medicine and Graduate School of Medicine, Hokkaido University, Kita 15, Nishi 7, Kita-ku, Sapporo 060-8638, Japan.

Tel: +81-117066978; Fax: +81-117067827

Email: takumaeda1105@yellow.plala.or.jp

Keywords: lymphedema, roxadustat, FG-4592, laboratory animal models

Abstract

Background*:* Lymphedema is an intractable disease with no curative treatment available. Conservative treatment is the mainstay, and new drug treatment options are strongly needed. The purpose of this study was to investigate the effect of roxadustat, a prolyl-4-hydroxylase inhibitor, on lymphangiogenesis and its therapeutic effect on lymphedema in a radiation-free mouse hindlimb lymphedema model.

***Methods and Results**:* Male C57BL/6N mice (8–10 weeks old) were used for the lymphedema model. Mice were randomized to an experimental group receiving roxadustat or a control group. The circumferential ratio of the hindlimbs was evaluated and lymphatic flow of the hindlimbs was compared by fluorescent lymphography up to 28 days postoperatively. The roxadustat group showed an early improvement in hindlimb circumference and stasis of lymphatic flow. The number and area of lymphatic vessels on postoperative day 7 were significantly larger and smaller, respectively, in the roxadustat group compared with the control group. Skin thickness and macrophage infiltration on postoperative day 7 were significantly reduced in the roxadustat group compared with the control group. The relative mRNA expression of hypoxia-inducible factor-1α (*Hif-1α*), vascular endothelial growth factor receptor-3 (*VEGFR-3*), vascular endothelial growth factor-C (*VEGF-C*), and Prospero homeobox 1 (*Prox1*) on postoperative day 4 were significantly higher in the roxadustat group compared with the control group.

***Conclusions**:* Roxadustat demonstrated a therapeutic effect in a murine model of hindlimb lymphedema via promotion of lymphangiogenesis through the activation of HIF-1α, VEGF-C, VEGFR-3, and Prox1, suggesting the potential of roxadustat as a therapeutic option in lymphedema.

Condensed Abstract

The therapeutic effects of roxadustat were investigated in a murine model of hindlimb lymphedema. Mice that received roxadustat showed early improvement in hindlimb circumference and stasis of lymphatic flow. In specimens harvested from the hindlimb, the number of lymphatic vessels was significantly larger and the area of the lymphatic vessels significantly smaller in mice that received roxadustat compared with control mice. The relative mRNA expression of *HIF-1α*, *VEGF-C*, *VEGFR-3*, and *Prox1* was significantly

higher compared with control mice, suggesting that roxadustat may be a promising therapeutic drug for the treatment of lymphedema.

Introduction

Lymphedema is a refractory condition caused by decreased lymphatic transport capacity and characterized by local interstitial fluid accumulation, inflammation, and fatty degeneration of connective tissue.[1] Symptoms include pain, fatigue, and recurrent infections due to compromised immunity, which significantly reduces patients' activities of daily living. It affects 200 million people worldwide[2] and is a major complication after treatment of solid tumors.

Current treatments for lymphedema primarily include compression therapy, manual lymphatic drainage, and other conservative therapies, rather than rebuilding the destroyed lymphatic system. Although lymphovenous anastomosis and vascularized lymph node transplantation have been reported to be effective for lymphedema, only specialized centers are able to perform these procedures and their effectiveness remains controversial.[3] The pathophysiology of lymphedema remains to be clarified, and there is an urgent need for new drug therapies.

Roxadustat, a novel hypoxia-inducible factor (HIF) prolyl 4-hydroxylase inhibitor, is of interest as a treatment for renal anemia in patients with chronic kidney disease. In addition, it has been reported that roxadustat exerts therapeutic effects on cutaneous wound healing,[4,5] cardiac disease,[6] retinal disease,[7] spinal cord injury,[8] Parkinson's disease,[9] and malignant tumor growth[10,11] by stabilizing HIF-1α expression. These findings the great therapeutic potential of Roxadustat in diseases related to HIF-1α signaling.

In murine lymphedema, lymphatic stasis and inflammation stabilize HIF-1α and result in high levels of HIF-1α expression, indicating that this is required for reparative

lymphangiogenesis.[12] HIF-1α has also been shown to promote lymphangiogenesis by inducing the expression of vascular endothelial growth factor receptor-3 (VEGFR-3) and vascular endothelial growth factor-C (VEGF-C) in lymphatic endothelial cells.[12,13] Although it has been reported that the deletion or inhibition of HIF-1α exacerbated edema in a murine model of tail lymphedema postoperatively,[12,14] HIF-1α stabilization has not been studied in an animal model of lymphedema. Therefore, in this study, the therapeutic effects of roxadustat were investigated in a murine model of hindlimb lymphedema that we previously developed.[15]

Materials and Methods

Cell culture and treatment

Endothelial Cell Basal Media MV2 (PromoCell, Heidelberg, Germany) supplemented with and penicillin-streptomycin and Growth Medium MV2 Supplement Mix (PromoCell) was used to culture human dermal lymphatic endothelial cells (HDLECs) (PromoCell), and the HDLECs from passages 3–5 were used. Roxadustat (Selleck Chemicals, Houston, TX) was dissolved in dimethyl sulfoxide (DMSO) and added to the medium at final concentrations of 0, 5, 10, and 25 μM.

Proliferation assay

To assess the effect of roxadustat on HDLEC proliferation, a Cell Counting Kit-8 assay (CCK-8; Dojindo Molecular Technologies, Japan) was performed, following a previously reported protocol.[4] Briefly, cells were seeded on a 96-well plate at a density of 2×10^3 cells/well with 0, 5, 10, or 25 μM of roxadustat added to the medium and incubated for 5 days. From days 0–5, 10 μL of CCK-8 solution was added to each well, after which the

samples were incubated for 60 min at 37°C. The absorbance was detected at 450 nm on the Infinite 200 PRO microplate reader (Tecan Japan, Kawasaki, Japan).

Scratch wound assay

HDLECs were seeded in six-well plates at a density of 5.0×10^5 cells/well and cultured at 37°C for 24 h. After a confluent monolayer formed, a sterile pipette tip was used to make a linear scratch. Phosphate-buffered saline was used to wash away the cellular residue, after then 2 mL of medium containing 0, 5, 10, or 25 μM roxadustat was added to each well and the plates were incubated at 37°C. Photographs were taken at 0 and 24 h, and the amount by which each scratch had closed and the migration rate were determined using ImageJ software (National Institutes of Health, Bethesda, MD).

Tube formation assay

Pretreatment of HDLECs with 0, 5, 10, or 25 μM roxadustat was carried out for 24 h. Then, the HDLECs were mixed with medium and seeded in a 24-well plate precoated with 100 μL of Geltrex (Life Technologies, Grand Island, NY) at 8×10^4 cells/well and incubated at 37°C for 6 h. After microscopic observation, the total length of each tube was calculated using ImageJ software (National Institutes of Health).[4]

Animals

All experiments involving animals in this study were approved by the Hokkaido University Institutional Animal Care and Use Committee. Male C57BL/6N mice, 8–10 weeks of age (SLC, Tokyo, Japan), were kept in a room maintained at 24°C under a 12-h light/dark cycle with free access to food and water.

Murine Model and Drug Administration

The murine model of hindlimb lymphedema was created using our previously established method.[15] Briefly, a circumferential incision was made in the left inguinal skin, followed by resection of the inguinal lymph node and surrounding fat pad. After tying the prenodal and postnodal lymphatic vessels, the popliteal lymph node and surrounding fat pad were resected. A 1-mm-thick silicone sheet was used to fashion a 3-mm-wide rectangular splint, which was then placed in the inguinal wound and affixed to the skin and underlying muscle. The mice were randomly assigned to either an experimental group receiving 25 mg/kg roxadustat (Selleck Chemicals) in DMSO[4,7] or a control group receiving only DMSO and were given intraperitoneal injections every 2 days, including the day of surgery, for up to 2 weeks. A total of 36 mice were used and sacrificed on day 28 (12 mice for edema assessment and fluorescence lymphatic imaging), on day 7 (12 mice for histology), and on day 4 (12 mice for RNA isolation).

Edema Assessment

Lymphedema formation in the hindlimb was evaluated quantitatively on days 0, 2, 4, 7, 10, 14, 17, 21, 24, and 28 after surgery (n = 6 per group), at which time the circumference of the musculotendinous junction of the gastrocnemius muscle was measured bilaterally, and the circumference ratio was calculated according to the following formula.

Circumference ratio = (Treated hindlimb circumference / Untreated hindlimb circumference) × 100%.

Fluorescence Lymphatic Imaging

Lymphatic structures in the hindlimbs of the control and roxadustat groups were compared by fluorescent lymphography every week for 4 weeks postoperatively (n = 6 per group). Prior to

imaging, isoflurane was used to anesthetize the mice and their residual fur was removed. A 5-μL volume of indocyanine green solution (2.5 mg/mL Diagnogreen in distilled water; Daiichi Sankyo Company, Ltd., Tokyo, Japan;) was subcutaneously injected into both paws with a 26-gauge needle. Imaging was performed indocyanine green using a near-infrared fluorescence camera system (Photodynamic Eye; Hamamatsu Photonics, Hamamatsu, Japan) 15 min after indocyanine green injection. The coverage of the fluorescent area (i.e., the dermal backflow at the thigh) was measured using ImageJ software (National Institutes of Health).

Histology

Six mice per group were sacrificed at 7 days after surgery and skin samples were obtained. To minimize the impact of inflammation due to wound healing, the samples were taken from an area 6 mm distal to the inguinal wound. Then, skin sections were fixed in 4% paraformaldehyde, embedded in paraffin, and subjected to immunohistochemical or Elastica–Masson staining. Immunohistochemical staining was carried out to evaluate lymphatic endothelial cells and macrophage infiltration. Sections were incubated overnight with antibodies against LYVE-1 (Abcam, Inc., Cambridge, MA) and F4/80 (Cedarlane, Burlington, Canada). Histofine (Nichirei, Tokyo, Japan), which was developed using 3,3′-diaminobenzidine, was used as the secondary antibody. Elastica–Masson staining was performed to evaluate skin thickness. A whole-slide scanner (Nano Zoomer Digital Pathology; Hamamatsu Photonics) was used to capture digital images of the slides, which were then visualized using NDP.view2 software (Hamamatsu Photonics). In accordance with a previous report,[16] lymphatic vessels were defined as vessels with an immunopositive endothelium and a vascular lumen. Lymphatic vessels were identified by two examiners other than the first author after the specimens were randomized, and those identified by both

examiners were designated as lymphatic vessels. LYVE-1-stained sections were scanned at low magnification (40×) and "hot spots" with the greatest number of lymphatic vessels were noted. Then, five of these areas in each section were observed at high magnification (200×) and the average number of lymphatic vessels within the hot spots in each field of view was calculated.[17] Additionally, the average area of the lymphatic lumen in each field of view was calculated using ImageJ software (National Institutes of Health). Quantification of the F4/80 positive area was performed using ImageJ software (National Institutes of Health) by observing 10 randomly selected high-magnification fields of view (400×). The thickness of skin in the roxadustat and control groups was measured as the distance from the epidermis to the dermal-fat junction by two examiners other than the first author, using ImageJ software (National Institutes of Health) after the specimens were randomized.

RNA Isolation and Real-Time Polymerase Chain Reaction

To isolate the RNA, 6 mice per group were sacrificed at 4 days after surgery. Skin and subcutaneous tissue samples were collected from the hindlimb at an area 6 mm distal to the inguinal wound and frozen. RNeasy Fibrous Tissue Mini Kit (Qiagen, Hilden, Germany) was used to extract total RNA from the skin samples, after which a High Capacity RNA-to-cDNA Kit (Applied Biosystems, Foster City, CA) was used to reverse-transcribe the RNA to cDNA. Next, Power SYBR Green PCR Master Mix and a StepOnePlus Real-Time PCR System (Applied Biosystems) were used to perform real-time quantitative reverse transcription polymerase chain reaction (PCR) and the relative levels of PCR products were calculated using the ΔΔCt method.[15] Examinations of each sample was were performed three times. Primers for reverse transcription PCR are listed in Table 1.

Statistical Analysis

Differences between the two groups were analyzed by Student's *t*-test, while differences among three or more groups were analyzed by one-way analysis of variance followed by a Tukey–Kramer multiple comparisons test. Results from multiple experiments are expressed as mean values ± standard error. All statistical analyses was performed using JMP software ver. 16.0.0 (SAS Institute, Inc., Cary, NC), with $p < 0.05$ considered to indicate statistical significance.

Results

In vitro assays

Roxadustat was found to stimulate the proliferation of HDLECs in a dose-dependent manner (Fig. 1A) and significantly enhanced their motility ($p < 0.05$) (Fig. 1B, C). Roxadustat also significantly enhanced HDLEC tube formation ($p < 0.05$) (Fig. 1D, E).

Edema Assessment

Edema disappeared grossly on days 21 and 28 in the roxadustat and control groups, respectively (Fig. 2A). The hindlimb circumference ratio reached a maximum on day 4 in both groups and then gradually approached 100%. As in our previous study,[15] the hindlimb circumference ratio reached 100% on day 28 in the control group and on day 21 in the roxadustat group. The circumference ratio was significantly lower in the roxadustat group compared with the control group from postoperative days 2–24 (Fig. 2B).

Fluorescence Lymphatic Imaging

The control group showed diffuse dermal backflow throughout the treated hindlimb from 1–4 weeks postoperatively. In contrast, the roxadustat group showed dermal backflow, but with lower fluorescence compared with the control group (Fig. 3A). Compared with the control

group, the coverage of the fluorescent area at the thigh at 2 weeks postoperatively was significantly reduced in the roxadustat group (*$p < 0.05$) (Fig. 3B).

Histology

The roxadustat group had more lymphatic vessels (Fig. 4A, B) and a smaller lymphatic lumen area (Fig. 4A, C) compared with control group. There were also significantly more LYVE-1-positive lymphatic vessels in the roxadustat group (8.5 ± 0.5) compared with the control group (5.2 ± 0.4) (Fig. 4B, $p < 0.05$). The area of lymphatic lumen in the roxadustat group (334 ± 38 μm^2) was significantly less than that in the control group (1,385 ± 163 μm^2) (Fig. 4C, $p < 0.05$). Furthermore, the F4/80-positive area was significantly smaller in the roxadustat group (1.9 ± 0.3 %) compared with the control group (3.1 ± 0.4 %) (*$p < 0.05$) (Fig. 5A, B). Skin thickness in the roxadustat group (240 ± 18 μm) was significantly less than that in the control group (296 ± 12 μm) (*$p < 0.05$) (Fig. 5C, D).

Real-Time PCR

The relative mRNA expression levels of *Hif-1α*, *VEGFR-3*, *VEGF-C*, and Prospero homeobox 1 (*Prox1*) were significantly higher in the roxadustat group (1.6 ± 0.2, 4.3 ± 0.7, 2.5 ± 0.3, and 2.8 ± 0.4, respectively) compared with the control group (Fig. 6, $p < 0.05$).

Discussion

In this study, we used a novel radiation-free murine model of hindlimb lymphedema, which we had previously developed.[15] The lack of appropriate animal models is one of the reasons why the elucidation of the pathogenesis of lymphedema has been hampered. Many studies of lymphedema in animal models have been conducted mainly in mouse-tail[12,14] and hindlimb edema models,[18,19] but because the mouse-tail edema model does not involve lymph-node

248 excision and many murine models of hindlimb edema use radiation, a suitable clinical
249 lymphedema animal model for molecular biological studies did not exist. Our lymphedema
250 model does not use radiation, thus eliminating its effects. In addition, the lymph node
251 excision model more closely mimics clinical lymphedema.

252 Although there have been several reports on the most appropriate circumferential
253 measurement site for hindlimb lymphedema, including a point located at 5 or 6 mm from the
254 heel,[15,18] we took circumferential measurements at the musculotendinous junction of the
255 gastrocnemius muscle to ensure anatomic consistency at each time point,[17] taking into
256 account the growth of the mice during the experiment, and evaluated it in comparison with
257 the untreated side.

258 The circumferential ratio, which indicates the degree of edema, improved faster in
259 the roxadustat group compared with the control group. Fluorescent imaging evaluation of
260 lymphatic flow showed significantly lower fluorescence after 2 weeks in the roxadustat
261 group, whereas dermal backflow, which is indicative of lymphatic stasis, was diffuse
262 throughout the hindlimb over the 4-week postoperative period in the control group,
263 suggesting that lymphatic stasis was improved in the roxadustat group. Yamamoto et al.[20]
264 reported that the degree of dermal backflow was positively correlated with clinical severity,
265 and the present results are consistent with theirs. The formation of lymphatic collateral
266 vessels and enhanced function of the draining collecting vessels were considered as possible
267 reasons for the reduced dermal backflow in the roxadustat group, but neither could be
268 confirmed in our study due to the low resolution of the fluorescence camera system.

269 Microscopically, dilation of lymphatic vessels has been reported in the early stages
270 of lymphedema,[21] and our previous study involving a murine model of hindlimb lymphedema
271 revealed cutaneous and subcutaneous lymphatic dilation.[15] In the present study, we found that
272 on postoperative day 7, the number of cutaneous and subcutaneous lymphatic vessels was

273 significantly larger and their lumen area was significantly smaller in the roxadustat group
274 compared with the control group. This suggests that lymphangiogenesis was more
275 pronounced in the roxadustat group and that the dilation of lymphatic vessels, which
276 indicates lymphatic stasis, was improved. In addition, skin thickness in the roxadustat group
277 was significantly less than that in the control group. Furthermore, significantly less
278 macrophage infiltration was found in the roxadustat group than in the control group, which is
279 consistent with previous reports.[22]

280 HIF-1 is a transcriptional activator of various genes that play a role in the adaptive
281 response of cells to hypoxia. Dysfunction in systems that regulate HIF-1 activity has been
282 implicated in the pathogenesis of malignancies and other diseases.[23] HIF-1 has a
283 heterodimeric structure comprising oxygen-sensitive HIF-1α and constitutively expressed
284 HIF-1β subunits. Under normoxic conditions, the ubiquitin–proteasome pathway rapidly
285 degrades the HIF-1α subunit following hydroxylation of proline residues by HIF prolyl-4-
286 hydroxylases.[7] The HIF system targets a wide range of genes, and in particular, increased
287 HIF expression via prolyl hydroxylation domain protein inhibitors such as roxadustat has
288 been reported to have therapeutic effects in cutaneous wound healing,[4,5] cardiac disease,[6]
289 retinal disease,[7] spinal cord injury,[8] Parkinson's disease,[9] and malignant tumors,[10,11] and is
290 attracting attention as a new pharmacological target.

291 HIF-1α promotes lymphangiogenesis by inducing VEGFR-3 and VEGF-C
292 expression in lymphatic endothelial cells[12,13] and by increasing VEGFR-3 expression through
293 the transcriptional activation of Prox1.[24] It has also been reported that inhibition or deletion
294 of HIF-1α exacerbates edema in a murine model of tail lymphedema postoperatively.[12,14]
295 These findings suggest that HIF-1α expression may be involved in postoperative lymphatic
296 regeneration. In the present study, *Hif-1α*, *VEGFR-3*, *VEGF-C*, and *Prox1* mRNA expression
297 levels were significantly elevated in the roxadustat group, suggesting that roxadustat

298 stabilizes *Hif-1α* expression and promotes lymphangiogenesis via the increased expression of
299 *VEGFR-3*, *VEGF-C*, and *Prox1*.

300 VEGF-C is a critical regulator of lymphangiogenesis and controls numerous
301 lymphatic cell processes via VEGFR-3 signaling, including differentiation, migration, and
302 survival.[25] It has been shown that the local administration of VEGF-C or gene therapy
303 involving adenoviral vectors significantly increases lymphangiogenesis and decreases
304 swelling in animal models of both primary and secondary lymphedema.[26,27] However, the
305 application of VEGF-C therapy in the clinical setting has yet to be realized because VEGF-C
306 acts as a key regulator of the tumor microenvironment, potentially increasing the risk of
307 recurrence and metastasis.[25,28]

308 Previous studies have reported that Roxadustat is noncarcinogenic[29] and it was found
309 not to promote the initiation, progression, or metastasis of tumors in a VEGF-sensitive
310 spontaneous breast cancer model.[30] Meanwhile, a phase 2 study is being conducted to
311 evaluate roxadustat for the treatment of anemia in patients receiving chemotherapy for non-
312 myeloid malignancies (NCT04076943). In addition, there are reports that roxadustat inhibits
313 tumor growth by enhancing macrophage phagocytosis of malignant tumors[10] and by
314 increasing sensitivity to chemotherapy and inhibiting tumor growth in a murine model of
315 malignancy.[11] Although roxadustat is reported to have anti-tumor effects as described above,
316 an increase in *VEGF-C* mRNA expression was also found in the present study, and thus its
317 effects on malignant tumors warrant further study.

318 The present study has some limitations that merit consideration. First, the murine
319 model of hindlimb lymphedema examined in this study does not address chronic
320 lymphedema and is based on acute lymphedema. Human lymphedema progresses slowly and
321 does not improve spontaneously, whereas in animal models, it often resolves spontaneously.
322 In this model, gross edema resolves in approximately 1 month. Therefore, although this

model anatomically approximates human lymphedema, it is not a perfect mimic, including the course of the disease. Second, although data in numerous animal studies have demonstrated that roxadustat does not induce carcinogenesis[29] or promote cancer,[30] further safety verification through clinical trials is needed to ensure its safety against malignant tumors in the clinical context.

Conclusions

In summary, roxadustat exerted a therapeutic effect in a murine model of hindlimb lymphedema by promoting lymphangiogenesis via activation of HIF-1α, VEGFR-3, VEGF-C, and Prox1. This suggests that roxadustat induces reparative lymphangiogenesis against impaired lymphatic function and thus shows promise as a therapeutic option for lymphedema.

Acknowledgments

The authors would like to thank Kohei Oashi and Daisuke Iwasaki for advice regarding this study.

Author Contributions

Yoshitada Hoshino: Conceptualization, Investigation, Data curation, Writing- Original draft preparation

Masayuki Osawa: Methodology, Funding acquisition

Emi Funayama: Methodology, Validation

Kosuke Ishikawa: Supervision, Data curation

Takahiro Miura: Validation, Visualization

Masahiro Hojo: Data curation, Formal analysis

Yuhei Yamamoto: Conceptualization, Project administration

Taku Maeda: Conceptualization, Investigation, Supervision, Validation

Author Disclosure Statement

No competing financial interests exist.

Funding

This study was funded by the Japan Society for the Promotion of Science (Grant No. JP20K09841).

References

1. Alitalo K, Tammela T, Petrova TV. Lymphangiogenesis in development and human disease. Nature 2005;438(7070):946-953; doi: 10.1038/nature04480
2. Grada AA, Phillips TJ. Lymphedema: Pathophysiology and clinical manifestations. J Am Acad Dermatol 2017;77(6):1009-1020; doi: 10.1016/j.jaad.2017.03.022
3. Kong X, Du J, Du X, et al. A meta-analysis of 37 studies on the effectiveness of microsurgical techniques for lymphedema. Ann Vasc Surg 2022; doi: 10.1016/j.avsg.2022.04.038
4. Zhu Y, Wang Y, Jia Y, et al. Roxadustat promotes angiogenesis through HIF-1alpha/VEGF/VEGFR2 signaling and accelerates cutaneous wound healing in diabetic rats. Wound Repair Regen 2019;27(4):324-334; doi: 10.1111/wrr.12708
5. Tang D, Zhang J, Yan T, et al. FG-4592 Accelerates cutaneous wound healing by epidermal stem cell activation via HIF-1alpha stabilization. Cell Physiol Biochem 2018;46(6):2460-2470; doi: 10.1159/000489652
6. Deguchi H, Ikeda M, Ide T, et al. Roxadustat markedly reduces myocardial ischemia reperfusion injury in mice. Circ J 2020;84(6):1028-1033; doi: 10.1253/circj.CJ-19-1039
7. Liu H, Zhu H, Li T, et al. Prolyl-4-hydroxylases inhibitor stabilizes HIF-1alpha and increases mitophagy to reduce cell death after experimental retinal detachment. Invest Ophthalmol Vis Sci 2016;57(4):1807-1815; doi: 10.1167/iovs.15-18066
8. Wu K, Zhou K, Wang Y, et al. Stabilization of HIF-1alpha by FG-4592 promotes functional recovery and neural protection in experimental spinal cord injury. Brain Res 2016;1632:19-26; doi: 10.1016/j.brainres.2015.12.017
9. Li X, Cui XX, Chen YJ, et al. Therapeutic potential of a prolyl hydroxylase Inhibitor FG-4592 for Parkinson's diseases in vitro and in vivo: Regulation of redox biology and mitochondrial function. Front Aging Neurosci 2018;10:121; doi: 10.3389/fnagi.2018.00121

10. Nishide S, Matsunaga S, Shiota M, et al. Controlling the phenotype of tumor-infiltrating macrophages via the PHD-HIF axis inhibits tumor growth in a mouse model. iScience 2019;21:205; doi: 10.1016/j.isci.2019.10.031
11. Koyama S, Matsunaga S, Imanishi M, et al. Tumour blood vessel normalisation by prolyl hydroxylase inhibitor repaired sensitivity to chemotherapy in a tumour mouse model. Sci Rep 2017;7:45621; doi: 10.1038/srep45621
12. Zampell JC, Yan A, Avraham T, et al. HIF-1alpha coordinates lymphangiogenesis during wound healing and in response to inflammation. FASEB J 2012;26(3):1027-1039; doi: 10.1096/fj.11-195321
13. Han T, Yan J, Chen H, et al. HIF-1alpha contributes to tube malformation of human lymphatic endothelial cells by upregulating VEGFR-3. Int J Oncol 2019;54(1):139-151; doi: 10.3892/ijo.2018.4623
14. Jiang X, Tian W, Granucci EJ, et al. Decreased lymphatic HIF-2alpha accentuates lymphatic remodeling in lymphedema. J Clin Invest 2020;130(10):5562-5575; doi: 10.1172/JCI136164
15. Iwasaki D, Yamamoto Y, Murao N, et al. Establishment of an acquired lymphedema model in the mouse hindlimb: Technical refinement and molecular characteristics. Plast Reconstr Surg 2017;139(1):67e-78e; doi: 10.1097/PRS.0000000000002887
16. Kato T, Prevo R, Steers G, et al. A quantitative analysis of lymphatic vessels in human breast cancer, based on LYVE-1 immunoreactivity. Br J Cancer 2005;93(10):1168-1174; doi: 10.1038/sj.bjc.6602844
17. Hayashida K, Yoshida S, Yoshimoto H, et al. Adipose-derived stem cells and vascularized lymph node transfers successfully treat mouse hindlimb secondary lymphedema by early reconnection of the lymphatic system and lymphangiogenesis. Plast Reconstr Surg 2017;139(3):639-651; doi: 10.1097/PRS.0000000000003110
18. Oashi K, Furukawa H, Oyama A, et al. A new model of acquired lymphedema in the mouse hind limb: A preliminary report. Ann Plast Surg 2012;69(5):565-568; doi: 10.1097/SAP.0b013e31821ee3dd
19. Shioya R, Furukawa H, Murao N, et al. Prevention of lymphedematous change in the mouse hindlimb by nonvascularized lymph node transplantation. Ann Plast Surg 2016;76(4):442-445; doi: 10.1097/SAP.0000000000000428
20. Yamamoto T, Narushima M, Doi K, et al. Characteristic indocyanine green lymphography findings in lower extremity lymphedema: the generation of a novel lymphedema severity staging system using dermal backflow patterns. Plast Reconstr Surg 2011;127(5):1979-1986; doi: 10.1097/PRS.0b013e31820cf5df
21. Weber E, Agliano M, Bertelli E, et al. Lymphatic collecting vessels in health and disease: A review of histopathological modifications in lymphedema. Lymphat Res Biol 2022; doi: 10.1089/lrb.2021.0090
22. Miao AF, Liang JX, Yao L, et al. Hypoxia-inducible factor prolyl hydroxylase inhibitor roxadustat (FG-4592) protects against renal ischemia/reperfusion injury by inhibiting inflammation. Ren Fail 2021;43(1):803-810; doi: 10.1080/0886022X.2021.1915801
23. Koyasu S, Kobayashi M, Goto Y, et al. Regulatory mechanisms of hypoxia-inducible factor 1 activity: Two decades of knowledge. Cancer Sci 2018;109(3):560-571; doi: 10.1111/cas.13483
24. Zhou B, Si W, Su Z, et al. Transcriptional activation of the Prox1 gene by HIF-1alpha and HIF-2alpha in response to hypoxia. FEBS Lett 2013;587(6):724-731; doi: 10.1016/j.febslet.2013.01.053

25. Dayan JH, Ly CL, Kataru RP, et al. Lymphedema: Pathogenesis and novel therapies. Annu Rev Med 2018;69:263-276; doi: 10.1146/annurev-med-060116-022900
26. Hartiala P, Saarikko AM. Lymphangiogenesis and lymphangiogenic growth factors. J Reconstr Microsurg 2016;32(1):10-15; doi: 10.1055/s-0035-1544179
27. Baker A, Kim H, Semple JL, et al. Experimental assessment of pro-lymphangiogenic growth factors in the treatment of post-surgical lymphedema following lymphadenectomy. Breast Cancer Res 2010;12(5):R70; doi: 10.1186/bcr2638
28. Brown S, Dayan JH, Coriddi M, et al. Pharmacological treatment of secondary lymphedema. Front Pharmacol 2022;13:828513; doi: 10.3389/fphar.2022.828513
29. Beck J, Henschel C, Chou J, et al. Evaluation of the carcinogenic potential of roxadustat (FG-4592), a small molecule Inhibitor of hypoxia-Inducible factor prolyl hydroxylase in CD-1 mice and Sprague Dawley rats. Int J Toxicol 2017;36(6):427-439; doi: 10.1177/1091581817737232
30. Seeley TW, Sternlicht MD, Klaus SJ, et al. Induction of erythropoiesis by hypoxia-inducible factor prolyl hydroxylase inhibitors without promotion of tumor initiation, progression, or metastasis in a VEGF-sensitive model of spontaneous breast cancer. Hypoxia (Auckl) 2017;5:1-9; doi: 10.2147/HP.S130526

435 **Figure Legends**

436 **FIG. 1.** Effects of roxadustat on human dermal lymphatic endothelial cells (HDLECs) *in*
437 *vitro*. **(A)** Roxadustat stimulated HDLEC proliferation in a dose-dependent manner. **(B)**
438 Effects of roxadustat on HDLEC migration. *Scale bar* = 200 μm. **(C)** Roxadustat
439 significantly enhanced HDLEC migration in a dose-dependent manner. *Error bars* = standard
440 error of the mean. **(D)** Effects of roxadustat on the HDLEC tube formation. *Scale bar* = 200
441 μm. **(E)** Roxadustat significantly enhanced HDLEC tube formation at concentrations of 10
442 and 25 μM. *Error bars* = standard error of the mean. **(A, C, E)** *$p < 0.05$ compared with the
443 control group, †$p < 0.05$ compared with the 5-μM roxadustat treatment group, ‡$p < 0.05$
444 compared with the 10-μM roxadustat treatment group.
445
446 **FIG. 2.** Effects of roxadustat on edema. **(A)** Representative images of the murine model of
447 hindlimb lymphedema in both groups. Hindlimb circumference was measured at the
448 musculotendinous junction of the gastrocnemius muscle (arrowhead). **(B)** Edema assessment
449 demonstrated that the roxadustat group had a lower circumference ratio than the control
450 group from postoperative days 2 to 24 (*$p < 0.05$). *Error bars* = standard error of the mean.
451
452 **FIG. 3.** Effects of roxadustat on lymphatic flow. **(A)** Representative images of fluorescent
453 lymphography in both groups at postoperative weeks 1–4. In the treated hindlimb,
454 fluorescence was observed extensively at the thigh (*area outlined in yellow*). The popliteal
455 lymph node (*arrowhead*) was identified in the untreated hindlimb. (**B)** The coverage of the
456 fluorescent area at the thigh in the roxadustat group was significantly less than that in the
457 control group at postoperative weeks 2–4 (*$p < 0.05$). *Error bars* = standard error of the
458 mean.
459

FIG. 4. Effects of roxadustat on lymphatic vessels. **(A)** Representative photomicrographs of LYVE-1 immunohistochemical staining in the control group (*left*) and the roxadustat group (*right*) at postoperative day 7. *Scale bars* = 250 μm. **(B)** The average number of lymphatic vessels was significantly larger in the roxadustat group compared with the control group (*$p < 0.05$). *Error bars* = standard error of the mean. **(C)** The average area of lymphatic vessels in the roxadustat group was smaller than that in the control group (*$p < 0.05$). *Error bars* = standard error of the mean.

FIG. 5. Effects of roxadustat on macrophage infiltration and skin thickness. **(A)** Representative photomicrographs of F4/80 immunohistochemical staining in the control group (*left*) and the roxadustat group (*right*) at postoperative day 7. *Scale bars* = 250 μm. **(B)** The F4/80-positive area in the roxadustat group was significantly less than that in the control group (*$p < 0.05$). *Error bars* = standard error of the mean. **(C)** Representative photomicrographs of Elastica–Masson staining in the control group (*left*) and the roxadustat group (*right*) at postoperative day 7. *Scale bars* = 250 μm. **(D)** Skin thickness in the roxadustat group was significantly less than that in the control group (*$p < 0.05$). *Error bars* = standard error of the mean.

FIG. 6. Real-time reverse transcription PCR analysis of the skin and subcutaneous tissues demonstrated that *Hif-1α*, *VEGF-C*, *VEGFR-3*, and *Prox1* were expressed at significantly higher levels in the roxadustat group compared with the control group at postoperative day 4 (*$p < 0.05$). *Error bars* = standard error of the mean.

483 **Table 1. Reverse-transcription PCR primer sequences and product size**

Gene	Accession number	Primer sequences	Size (bp)
Hif-1α	NM_010431.2	MA216271-F: TGCGTGCATGTCTAATCTGTTCC MA216271-R: AAGATTCTGACATGCCACATAGCTC	102
VEGF-C	NM_009506.2	MA241730-F: TGCTGCTGCACATTATAACACAGA MA241730-R: CGGACACACATGGAGGTTTAAAGA	149
VEGFR-3	NM_008029.3	MA227448-F: TGGGCGACAGGGTTCTCATA MA227448-R: GACATGGTGGCTCTGGTCTAACTC	85
Prox1	NM_008937.3	MA209433-F: AGCCAGTGTTTAATCTTTGCATCC MA209433-R: AACCATTTGCCTGCTCATTCC	145
GAPDH	NM_008084.3	MA050371-F: TGTGTCCGTCGTGGATCTGA MA050371-R: TTGCTGTTGAAGTCGCAGGAG	150

484

A

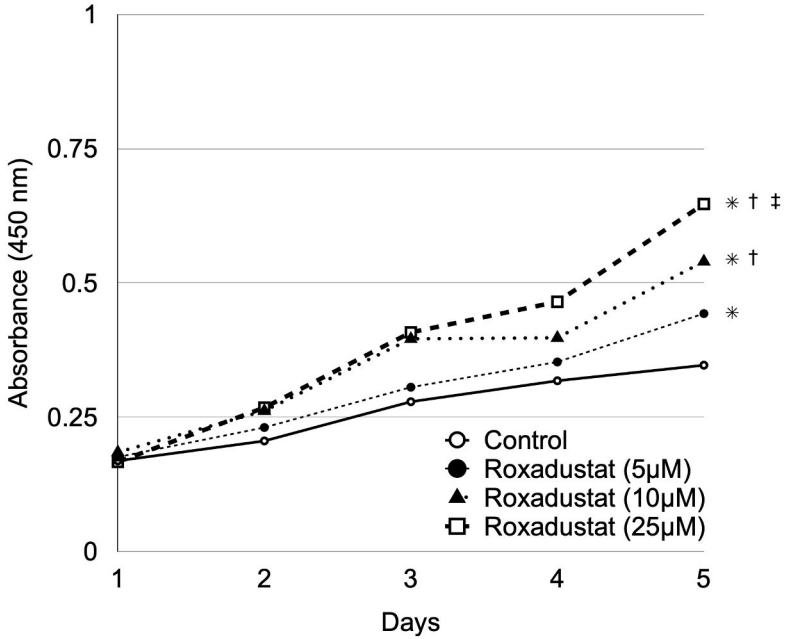
Absorbance (450 nm)
1
0.75
0.5
0.25
0
1
2
3
4
5
Days
Control
Roxadustat (5μM)
Roxadustat (10μM)
Roxadustat (25μM)
* † ‡
* †
*

B

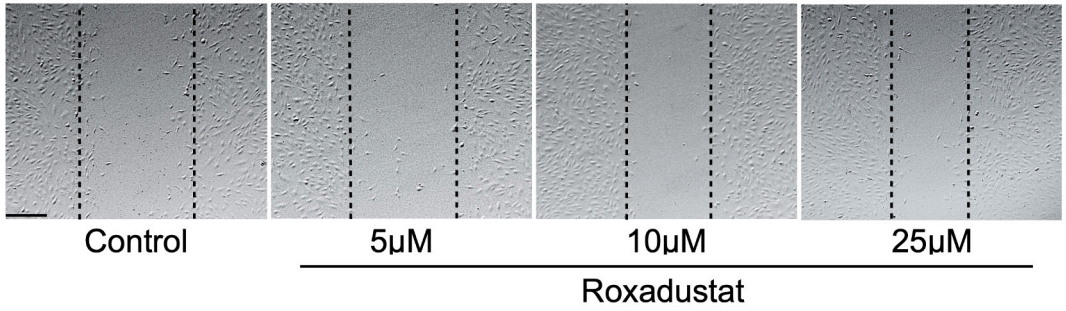
Control
5μM
10μM
25μM
Roxadustat

C

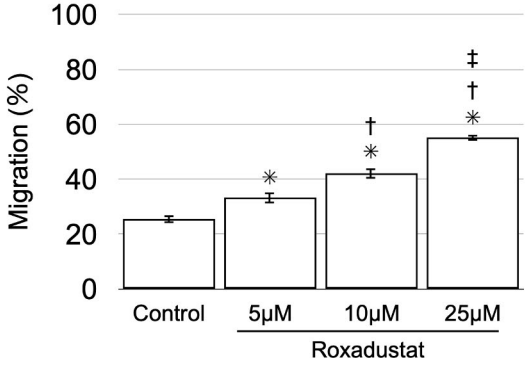
Migration (%)
100
80
60
40
20
0
Control
5μM
10μM
25μM
Roxadustat
‡
†
*

D

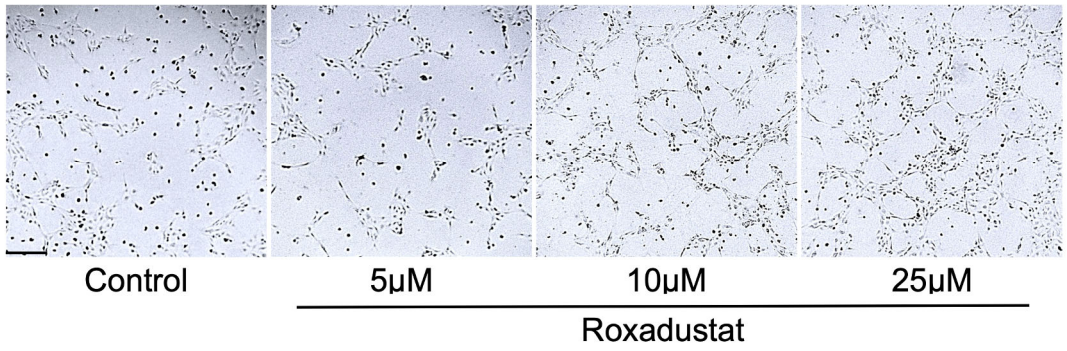
Control
5μM
10μM
25μM
Roxadustat

E

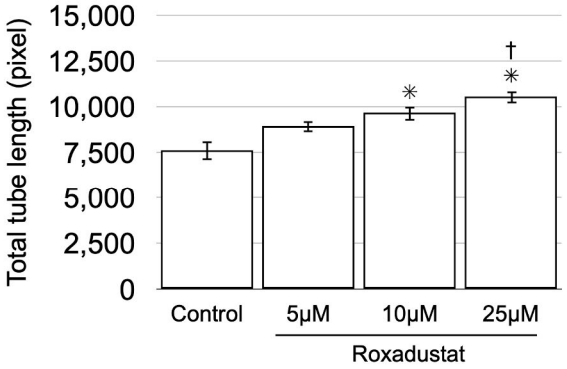
Total tube length (pixel)
15,000
12,500
10,000
7,500
5,000
2,500
0
Control
5μM
10μM
25μM
Roxadustat
†
*

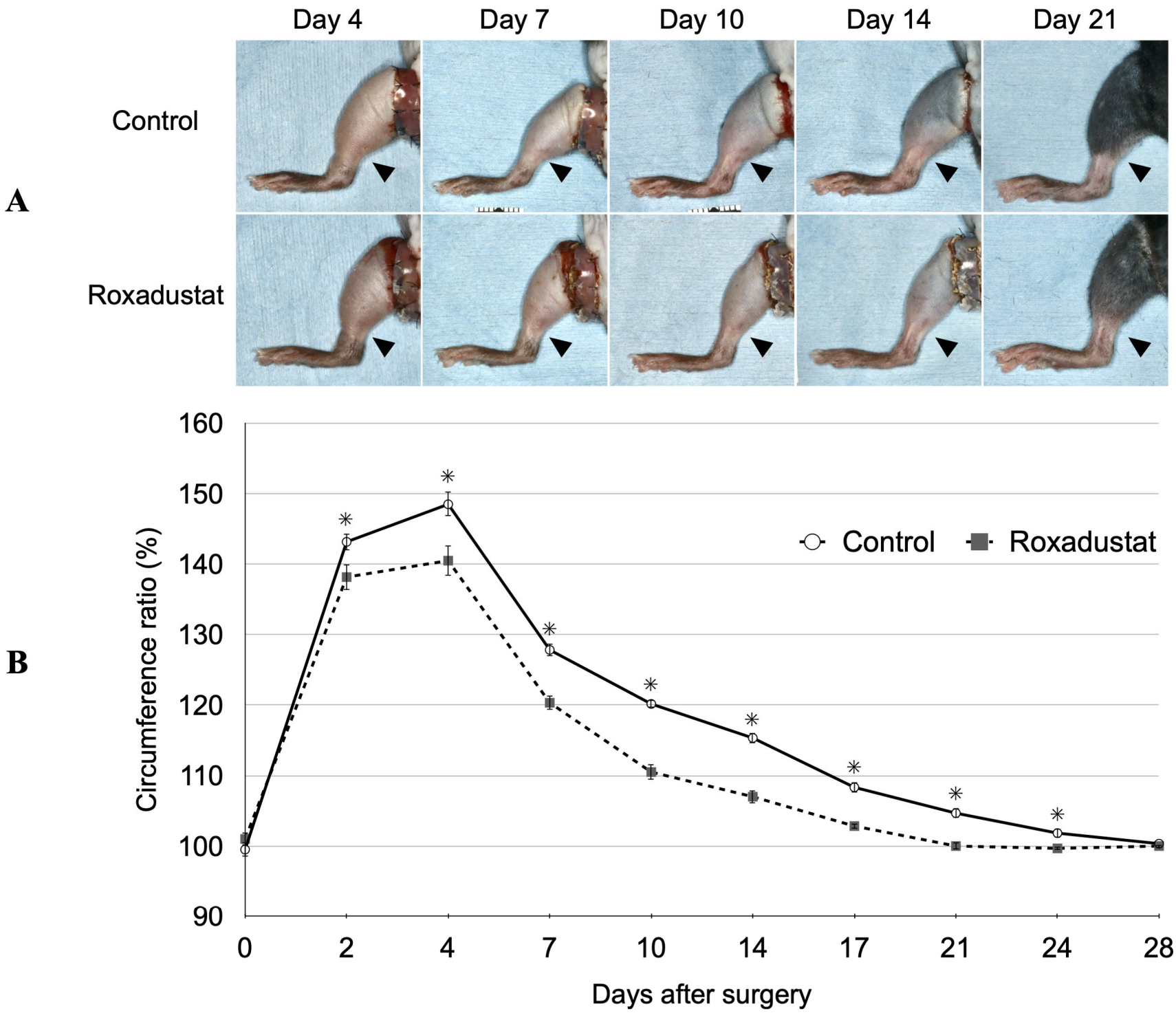
A
Day 4
Day 7
Day 10
Day 14
Day 21
Control
Roxadustat
B
Circumference ratio (%)
160
150
140
130
120
110
100
90
Control
Roxadustat
0
2
4
7
10
14
17
21
24
28
Days after surgery

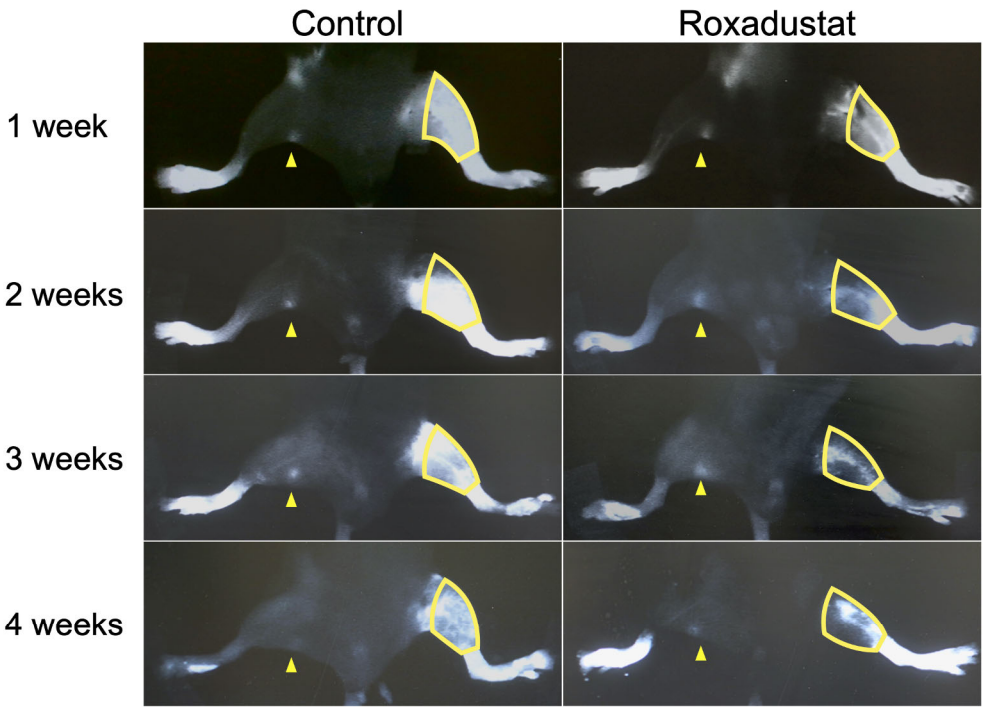
Control
Roxadustat
1 week
2 weeks
3 weeks
4 weeks

A

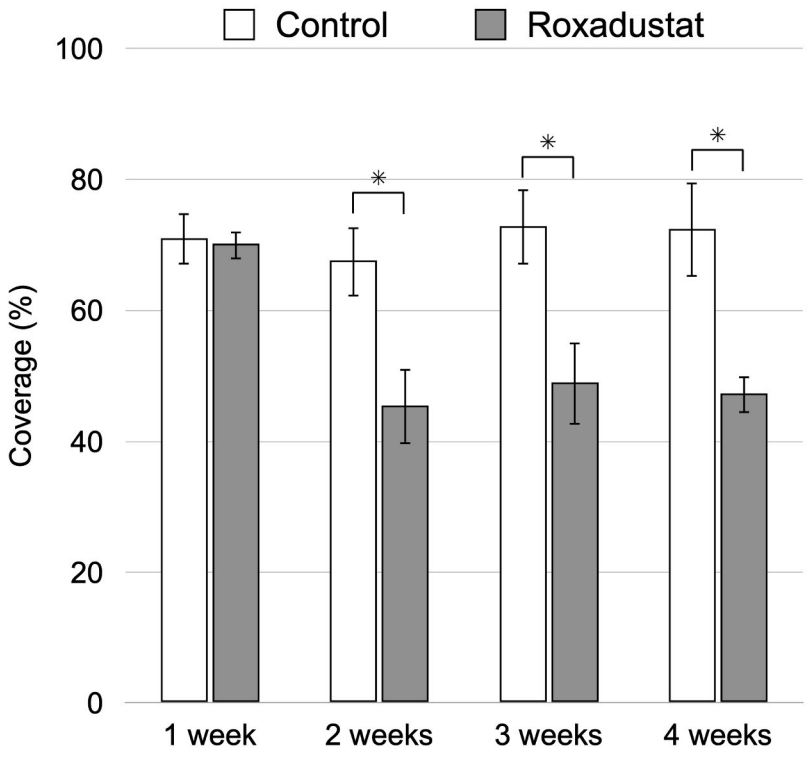
Control
Roxadustat
Coverage (%)
100
80
60
40
20
0
1 week
2 weeks
3 weeks
4 weeks
*
*
*

B

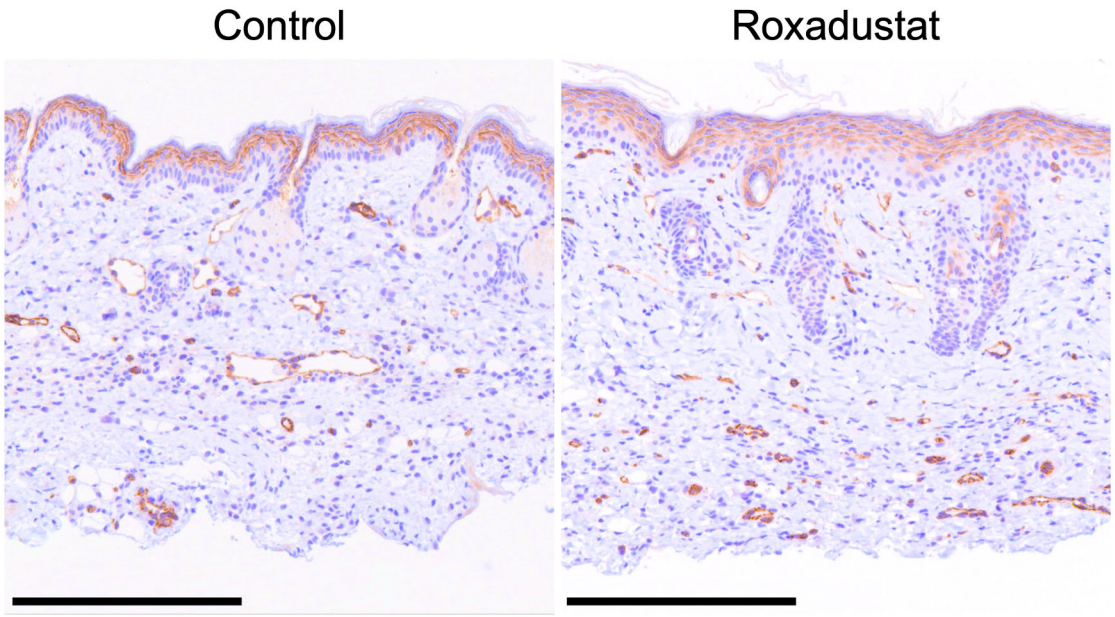
Control
Roxadustat

A

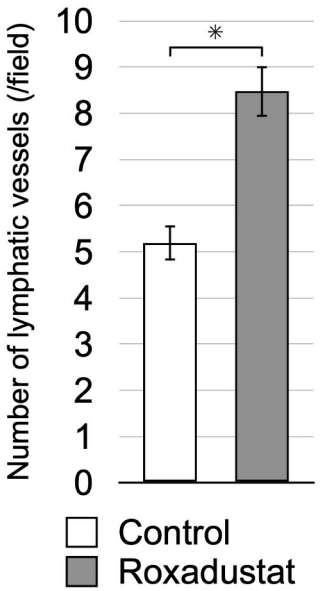
Number of lymphatic vessels (/field)
10
9
8
7
6
5
4
3
2
1
0
*
Control
Roxadustat

B

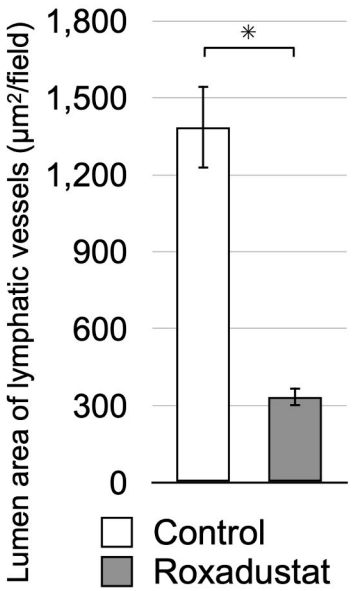
Lumen area of lymphatic vessels (μm²/field)
1,800
1,500
1,200
900
600
300
0
*
Control
Roxadustat

C

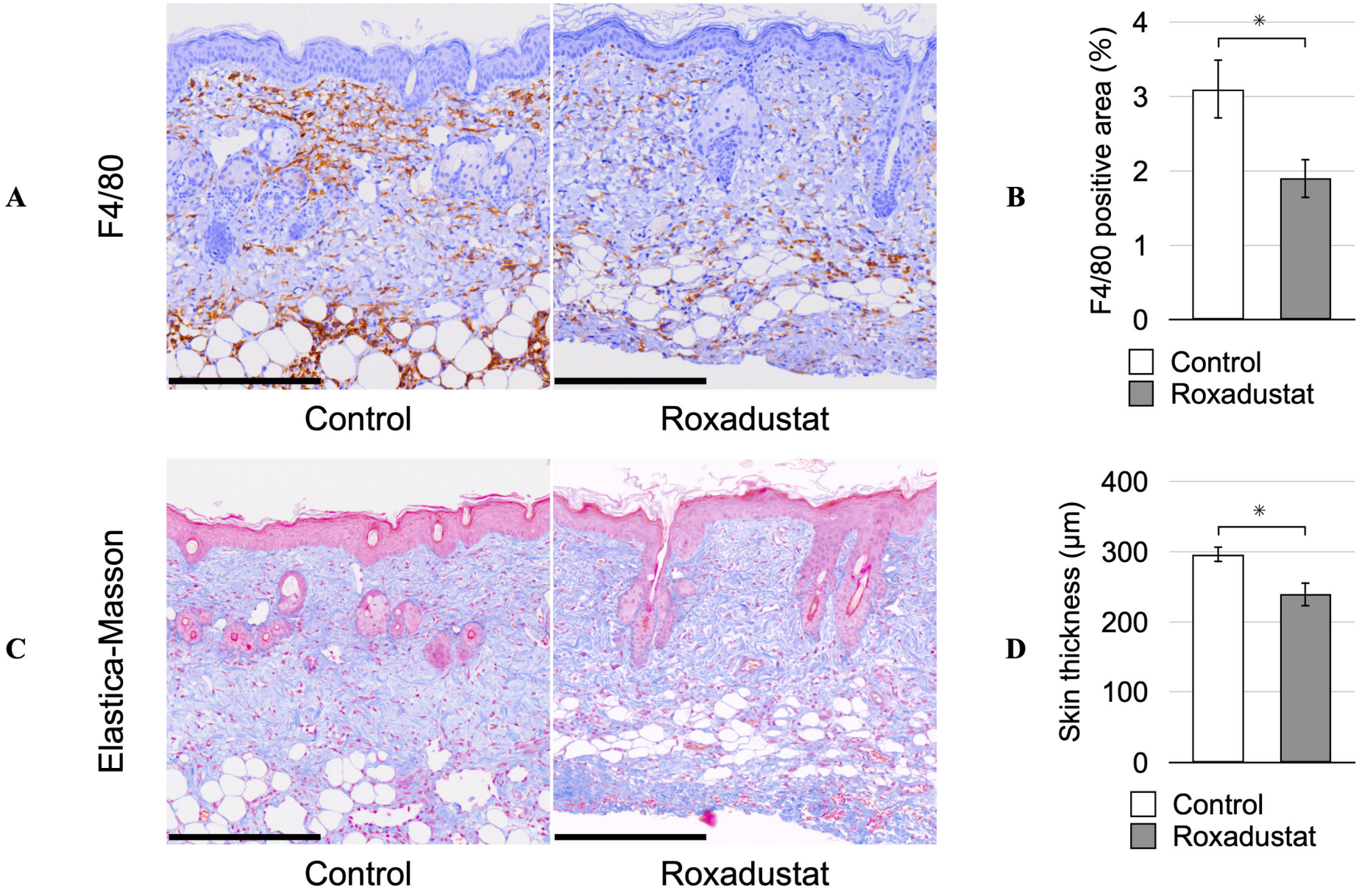
A
F4/80
Control
Roxadustat
B
F4/80 positive area (%)
4
3
2
1
0
*
Control
Roxadustat
C
Elastica-Masson
Control
Roxadustat
D
Skin thickness (μm)
400
300
200
100
0
*
Control
Roxadustat

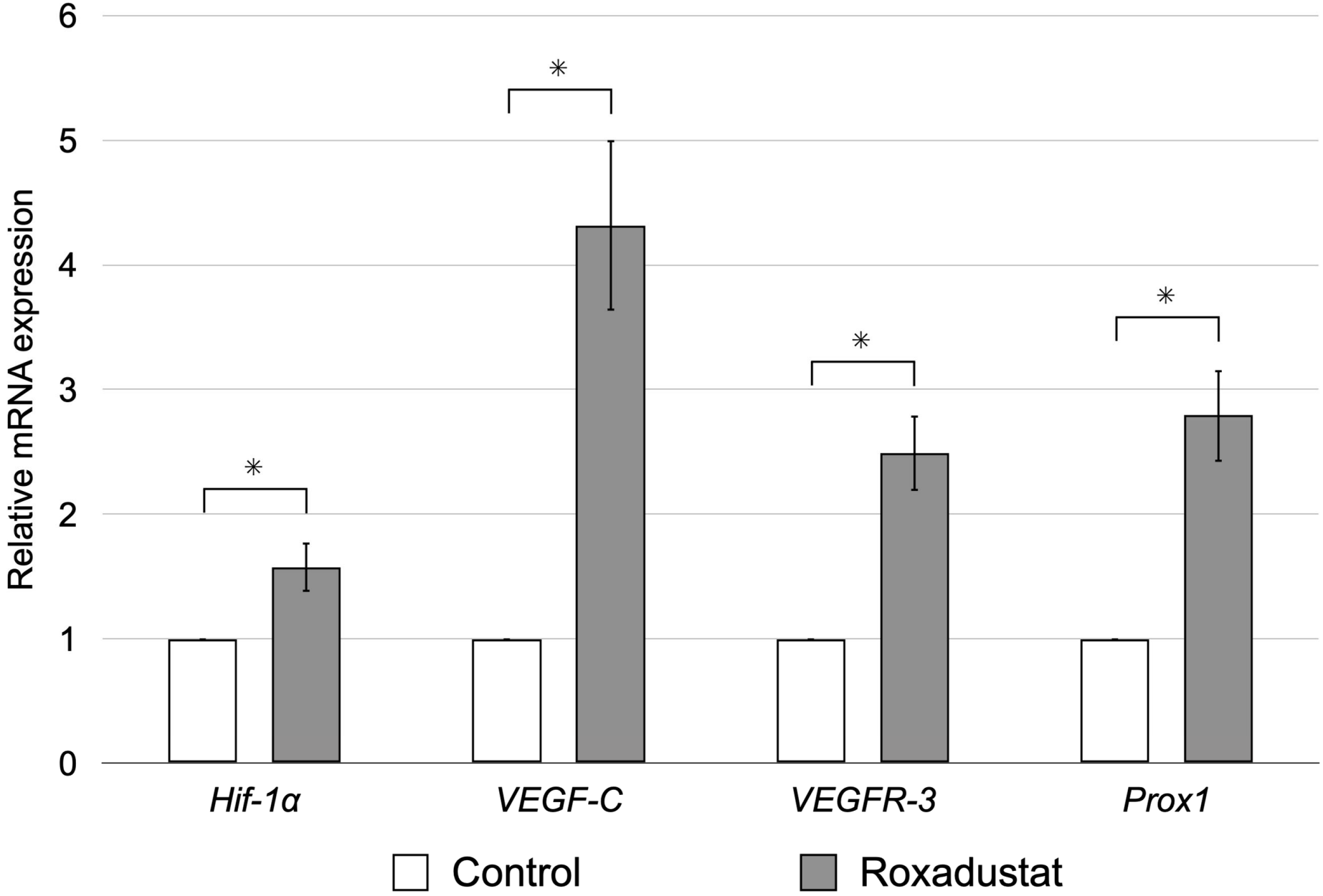
Relative mRNA expression
6
5
4
3
2
1
0
*
*
*
*
Hif-1α
VEGF-C
VEGFR-3
Prox1
Control
Roxadustat